JOURNAL
OF THE AMERICAN CHEMICAL SOCIETY

VOLUME 98, NUMBER 7 MARCH 31, 1976

Sulfuranes. Theoretical Aspects of Bonding, Substituent Site Preferences, and Geometrical Distortions

Maynard M. L. Chen and Roald Hoffmann*

Contribution from the Department of Chemistry, Cornell University, Ithaca, New York 14853. *Received July 1, 1975*

Abstract: A molecular orbital analysis of the electronic structure of sulfuranes, SR_4, finds many analogies to the phosphoranes. The basic picture is of electron-rich three-center bonding, with concomitant weakened axial bonds and electron-rich axial sites. The novel feature of the sulfuranes is a directional lone pair in the equatorial plane, which makes itself felt especially in setting conformational preferences for substituents bearing π-type electrons. The nonbonding orbital of the three-center bond and the S lone pair are of the same symmetry type. They mix and compete for position as the highest occupied molecular orbital of the molecule. Substituent site preferences for the SR_4 structure are the same as for the phosphoranes for σ effects, i.e., more electronegative substituents should enter the axial sites. For π effects the preferences are modified by the presence of the sulfur lone pair. Several conclusions are drawn concerning the interrelationship of axial substitution and the equatorial bond angle: (1) the difference in axial and equatorial bond strengths should lessen with increasing equatorial angle; (2) if the axial bonds are stretched, one expects the equatorial angle to decrease; (3) substitution in the axial positions by more electronegative ligands should favor a smaller angle between the equatorial ligands. Support for these conclusions is sought in assorted S, Se, and Te structures.

The prototype SR_4, sulfurane, structure is that of SF_4. As shown in **1**, the molecule has a C_{2v} geometry.[1] Other

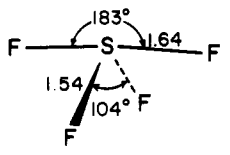

1

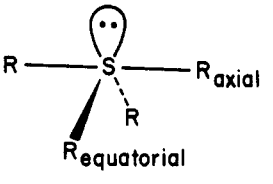

2

SR_4 and related Se and Te compounds show similar geometrical features.[2] The sulfurane structures are best described as close to a trigonal bipyramid geometry, with an equatorial lone pair, and distinguishable axial and equatorial sites, **2**.

It was pointed out by Muetterties and Schunn,[3] and subsequently confirmed by further structural studies of SR_4 compounds, that electronegative substituents prefer the axial sites and that these axial bonds are weak. Evidence for the bond weakening comes from the solid state bond lengths, which can exceed the sum of the covalent radii by as much as 0.25 Å.[4] Theories which can explain these observations have not been lacking. Some dealt directly with sulfuranes,[5] but many more were applied to the isoelectronic phosphoranes, interhalogen compounds, and xenon halides.[6] Several detailed molecular orbital calculations on sulfuranes have been published.[7] We present here a molecular orbital scheme based on extended Hückel calculations (computational details are given in the Appendix) which is consistent with the earlier work. We explore the consequences of substitution upon the equatorial angle, as well as the preferential orientation of π-donor and acceptor substituents.

The Orbitals of SH_4

The C_{2v} structure characteristic of sulfuranes is related in an obvious way to a square-planar geometry **3** and a tetrahedron **4**. Either extreme serves as a convenient starting

3 **4**

point for a discussion of the electronic structure of SH_4, and we have opted for the square-planar structure.[8] Figure 1 shows in an interaction diagram how the orbitals of a square-planar SH_4 are formed from the 3s and 3p orbitals of S and the symmetry-adapted H 1s combinations. Not surprisingly the construction matches that of another XH_4 system, square-planar methane.[9,10] In SH_4 all orbitals through the b_{1g} are occupied by the ten valence electrons. There is some uncertainty about the ordering of the two higher occupied orbitals, a_{2u} and b_{1g}. The former is entirely

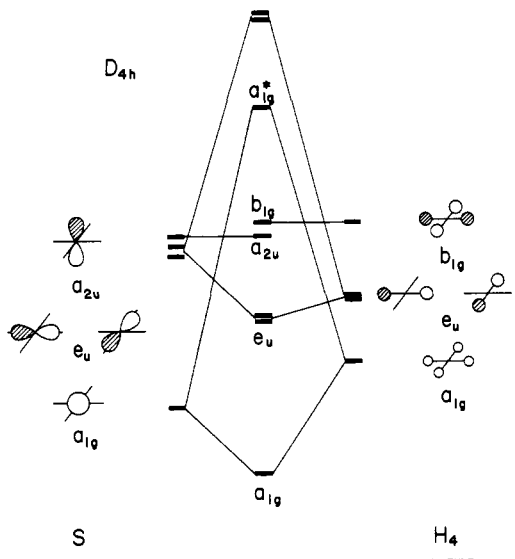

Figure 1. Interaction diagram for a square-planar (D_{4h}) SH_4.

on the central atom, the latter entirely on the ligands. The ordering of the two MO's could depend on the nature of the R group in SR_4.

We proceed to carry out the distortion indicated in **3**, bending two *trans* hydrogens down until they make an angle of 120°. Figure 2 traces the resultant energy changes. A similar analysis has been made by Gleiter and Veillard.[7h] Let us consider what happens to the bonding orbitals of the molecule. One member of the e_u set, the one along the axial direction, is unaffected by the distortion. The other e_u component, the one in the equatorial plane, loses bonding overlap between S 3p and H 1s, and turns on an antibonding interaction between the equatorial hydrogens. For both these reasons that e_u component, b_2 in C_{2v}, is destabilized.

In the lower symmetry of the C_{2v} geometry of SH_4 all levels which were of a_{1g}, a_{2u}, and b_{1g} symmetry in D_{4h} are reduced to a_1, and hence may interact. However, we find that in order to understand the qualitative changes in the two highest occupied orbitals, a_{2u} and b_{1g}, it is only necessary to introduce mixing with the unoccupied a_{1g}* level.[11]

The rules governing the phase relationships of orbitals as they mix, which we shall now make use of, are well-known.[12] Starting with the a_{2u}, pure $3p_z$, we begin the distortion of two trans hydrogens, downward in the *yz* plane. As the D_{4h} symmetry is lost, what was the b_{1g} level begins to mix into $3p_z$ in a bonding manner. (The b_{1g} is assumed to be at higher energy in the absence of any distortion.) The bonding relationship is here set by the $3p_z$-equatorial H overlap. The level moves down in energy. Conversely the p_z mixes into b_{1g} in an antibonding manner, pushing it up in energy. The resulting orbitals are represented schematically in **5**.

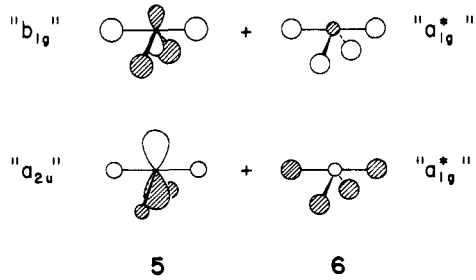

5 **6**

So far the mixing of the two filled levels causes neither differential accumulation of charge on the axial or equatorial hydrogens, nor a modification of the two bond types. These important effects can come about only through the secondary mixing with the empty a_{1g}*. Because that a_{1g}* is above both occupied levels, it will mix into them in a bonding way, i.e., bonding to the p_z component in each since the overlap between the components of the wave function located on the hydrogens is zero. **6** represents the contributions from this secondary mixing with the correct phase relative to **5**; summing **5** and **6** will give the orbitals displayed in Figure 2.

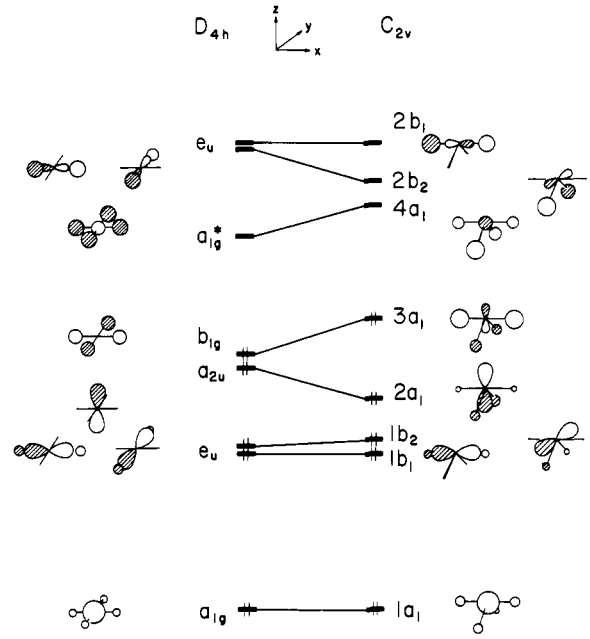

Figure 2. A schematic representation of the energy changes as a pair of trans hydrogens in D_{4h} SH_4 bend down, reducing their HSH angle from 180 to 120° to give the C_{2v} structure at the right.

The more one bends the equatorial hydrogens down, the more will the a_{1g}* orbital mix in. This is important, for it allows us to see how the composition of each orbital will change with bending. Take for instance the HOMO, made up by a superposition of the two contributions in the top row of **5** and **6**. The greater the mixing in of a_{1g}*, that is the greater the bending, the more concentrated is the HOMO wave function on the axial ligands. Also the more a_{1g}* mixes in, the more weakened are the axial bonds. Note that the mixing in of a_{1g}* cancels the equatorial density in b_{1g}, and thus negates the equatorial antibonding introduced by the first order mixing in that particular MO. It should be noted that this effect is a consequence of the mixing in of a_{1g}* and is independent of the initial (D_{4h}) ordering of the a_{2u} and b_{1g} orbitals.

The HOMO is, of course, a crucial orbital. Trends in it parallel, or better said, control, the electron density shifts in the molecule as a whole. That the HOMO should be more concentrated on the axial ligands and have weaker axial bonds as one lowers the equatorial angle is a fact that we will use later in our analysis.

The composition of the occupied molecular orbitals of SH_4, as they emerge from an extended Hückel calculation which omits 3d orbitals, is shown in Table I.

A question that might be asked of the calculations is whether the HOMO is the sulfur lone-pair orbital. In typical fashion the MO wave functions do not give an unequivocal answer, since there are varying S 3s and S $3p_z$ contributions smeared out over $1a_1$, $2a_1$, and $3a_1$. If a formal assignment must be made, $2a_1$ would be the orbital likely to be labeled as the lone pair, because of the large S $3p_z$ contribution in it.

A comparison of our results with a recent SCF calculation[7g,13] shows generally good agreement on the ordering

Table I. Molecular Orbitals of SH_4

Atomic orbitals	Molecular orbitals				
	$3a_1$	$2a_1$	$1b_2$	$1b_1$	$1a_1$
S s	−0.3991	−0.1794			0.7321
x				−0.4702	
y			−0.4873		
z	−0.5632	−0.6439			0.0027
H_{ax}	0.6260	−0.2682		±0.4903	0.1838
H_{eq}	−0.2307	0.4121	±0.5022		0.1849

of the MO levels and the relative magnitude of the AO coefficients. The only difference in ordering is in the b_1 and b_2 levels. From our derivation of the SH_4 levels it was clear why the b_2, because of the loss of overlap between the p_y and the equatorial hydrogens, must be raised above the b_1 in energy. By the same token we do not find it surprising that the relative ordering of b_1 and b_2 is not the same for different calculations. In our distortion to the C_{2v}, we preserved the same axial and equatorial bond distances. Schwenzer and Schaeffer[7g] calculate the equilibrium axial bond lengths of SH_4 longer by 0.35 Å. Undoubtedly, if we allowed the axial bond lengths to stretch, the same kind of destabilization would take place in b_1 because of the poorer overlap between $3p_x$ and the axial hydrogens. The relative energies of b_1 and b_2 should be a sensitive function of the assumed geometry.

Schwenzer and Schaeffer's results also suggest that the HOMO is mainly delocalized over the hydrogens, especially the axial ones, and that the second highest MO (our $2a_1$, their $5a_1$) is formally a lone pair on sulfur. That the extended Hückel calculation should give this is fortuitous since the character of the HOMO (the relative magnitudes of sulfur or hydrogen atomic orbital coefficients, but not the relative phase) will depend on the sulfur H_{ii} parameters. If the a_{2u} occurs above the b_{1g}, the HOMO will have greater density on the sulfur. We confirmed this point by changing the Coulomb integral of the sulfur atom, which essentially models a change in the electronegativity of the central atom. SCF and EH calculations on PH_4 show a similar effect.[8] Still another way to achieve an interchange in HOMO character is to lower the a_{2u} with highly electronegative substituents. Barring any gross changes brought about by the π interactions which we have not considered so far, we expect SF_4 to have a HOMO which is primarily sulfur lone pair in character.

Perhaps it is worthwhile to restate the conclusion that emerges from our analysis. In a localized, simplified picture of AR_4 molecules we expect to see at high energy an A atom lone pair in the equatorial plane and the nonbonding orbital of the electron-rich three-center bond. The calculations show that these two orbitals, both a_1 in C_{2v}, mix strongly. The primary character of the HOMO, that is whether it is the lone pair or the axial three-center bond nonbonding orbital, depends on the relative electronegativities of the central atom and its ligands.

Why do SR_4 molecules assume the C_{2v} structure? Departure from a tetrahedral geometry, not discussed in detail here, is assured by the level ordering of a tetrahedral XH_4 or XY_4 system.[10] Two orbitals, a_1 and t_2, compete for the highest energy electron pair in tetrahedral SH_4. The movement toward a C_{2v} structure is understandable as a first-order or second-order Jahn-Teller distortion,[14,15a] depending on whether t_2 or a_1 is at lower energy. Departing from the square planar D_{4h} extreme, our level scheme does not provide an obvious second-order Jahn-Teller rationale for distorting to C_{2v}.[15b] Falling back on the phenomenological aspects of the Walsh diagram of Figure 2, we note that the tendency to bend or not bend is set by the opposing slopes of the $2a_1$ and $3a_1$ levels. The balance is a delicate one; for instance our particular parameters favor a square-planar molecule. With other assumptions for the Coulomb integrals, bending results. One also gets bending if a length differential between the axial and equatorial bonds is introduced. For instance for S–H equatorial 1.35 Å and S–H axial 1.70 Å (the optimized lengths of Schwenzer and Schaeffer[7g]) EH gives an optimum equatorial angle of approximately 100°. It might be noted that the geometry of the nonexistent SH_4 is not known and that there is some disagreement on its equilibrium structure between calculations considerably better than our own. An ab initio calculation by Gleiter and Veillard,[7h] of roughly comparable quality to that cited earlier by Schwenzer and Schaeffer,[7g] yields an optimum C_{4v} structure, a flat square pyramid. A calculation of SF_2H_2 by Gleiter and Veillard[7h] results in a geometry close to the experimental SF_4 structure.

It may be noted from the Walsh diagram of Figure 2 that molecules with two less or two more electrons should introduce an energy factor favoring the square-planar geometry. Two less electrons get us to SiH_4 and the large family of group 4 tetracoordinate molecules. These, of course, prefer a tetrahedral geometry, not a square-planar one. The square-planar tetrahedral choice is made on another, well-known, slice of the XH_4 potential energy surface.[9,10] Two more electrons, i.e., 12 valence electrons, bring us to XeF_4, square planar, or more directly related to the molecules of interest, to the well-established family of square-planar Te(II) compounds.[16]

Axial vs. Equatorial Substituent Site Preferences and Bond Strengths

The analysis of the previous section affirms the basic picture of an axial electron-rich three-center bond system in sulfuranes, perturbed only by a mixing of the sulfur equatorial lone pair with the nonbonding orbital of the three-center orbital set. This mixing does not change the basic conclusions of the three-center picture: the axial bonds should be weaker than the equatorial ones, and electronic density should accumulate on the axial ligands.[5,6,17] The results of a Mulliken population analysis on SH_4 and SF_4 are shown in **7** and **8**. These numbers come from calculations without

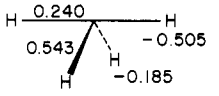

7

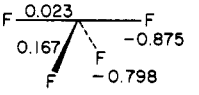

8

3d orbitals. The inclusion of 3d orbitals strengthens both axial and equatorial bonding and equalizes the charge distribution in the molecules.

From the charge distribution it follows that more electronegative substituents will enter the axial sites, quite analogous to the phosphorane case. This conclusion was checked by actual calculations replacing one or two hydrogens by more electronegative atoms.

The Interrelationship of Axial Substitution and Equatorial Angle

The derivation of the C_{2v} SH_4 orbitals by distortion from a D_{4h} structure was more than a pedagogical exercise. It allowed us to show, first, that the changes in the HOMO, accumulation of density on the axial atoms, relative weakening of the axial bonds, determined the similar effects in the molecule as a whole and, second, that the magnitude of

such changes was inversely related to the equatorial angle. Several interesting corollaries follow.

(1) The Difference in Axial and Equatorial Bond Strengths Should Lessen with Increasing Equatorial Angle. This is rather obvious and should not be difficult to test with bidentate ligands of varying size. Of pertinence in this regard is the series of tellurium diiodides[2h,j-m] where the axial atoms are iodines and the equatorial ones are carbons. Unfortunately, as pointed out by Knobler, McCullough, and Hope,[2m] it is hazardous to compare the Te–I bond distances because of the secondary bonding between the iodines of one molecule and the tellurium of another. $I_2Te(C_{12}H_8)$ which has the smallest equatorial angle (82°) has an average Te–I distance of 2.94 Å and is not the longest as expected. $I_2Te(C_{12}H_6O)$ with an equatorial angle of 91.5° also has a Te–I distance of 2.94 Å.

(2) Conversely, if the Axial Bonds Are Stretched, We Expect the Equatorial Angle to Decrease. There is some fragmentary experimental and theoretical evidence on this conclusion. The anthropomorphic axial bond stretching is a difficult task to accomplish in a controlled manner, but we can view SR_2 molecules in an unorthodox way as SR_4 with the axial atoms separated to infinity. The FSF angle in SF_2, 98°,[18] is smaller than the equatorial angle of 102–104° in SF_4.[1] The SCF optimization of SH_2 and SH_4 geometries[7g] predicts angles of 96 and 106°, respectively.

An interesting experimental example is the structure of 1-thia-4-selenacyclohexane 4,4-dibromide (**9**).[2n] Though a

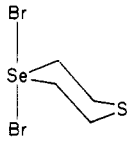

9

structure of 1-thia-4-selenacyclohexane is lacking, one might have expected approximately equal angles at S and Se in such a compound. This expectation is based on either a typical Bent[19] or Walsh[20] argument for the dependence of the RXR angle on the electronegativity of the central X atom or the experimental observation of a similar angle at Se in 1,4-diselenacyclohexane,[21] 98°, as in 1,4-dithiacyclohexane,[22] 99°. While the angle at the two-coordinate sulfur in the 1-thia-4-selenacyclohexane 4,4-dibromide is normal, 97°, the equatorial angle at the four-coordinate selenium opens up to 108°.[27]

Incidentally, there is another neat way to reach the basic conclusions (1) and (2). This begins from a construction of the orbitals of C_{2v} SH_4 from SH_2 and two axial hydrogens, given in the self-explanatory form of Figure 3, also presented by Gleiter and Veillard.[7h] Let us assign the electrons of the two incoming hydrogens more or less arbitrarily to the a_1 orbital at infinite separation. As the two hydrogens approach closer to SH_2, the interaction between the various a_1 orbitals grows. The only interaction among a_1 orbitals that has bonding consequences is that between the occupied a_1 descended from the axial hydrogens and the unfilled, antibonding a_1* of SH_2, the highest orbital shown for that fragment. The lower that a_1* is in energy, the greater its stabilizing mixing into the axial hydrogen a_1 combination. The energy of the a_1* is nicely lowered by increasing the equatorial HSH angle in the SH_2 fragment. That distortion decreases the strongly antibonding overlap between the sulfur p orbital and the equatorial hydrogens in that orbital. Our chain of reasoning thus associates an increasing equatorial angle with a greater interaction with the axial hydrogens or a shorter, stronger axial bond.

Table II. Selected X_2AY_2 Structures

Compd	Equatorial angle	Ref
$(OR)_2SPh_2$	104.4	2b
$Cl_2S(C_6H_4Cl)_2$	108.6	2c
$Cl_2Se(C_6H_4CH_3)_2$	106.5	2e
$Br_2Se(C_6H_4CH_3)_2$	108.0	2e
Br_2TePh_2	94.4	2g
$I_2Te(C_6H_4Cl)_2$	101.1	2h

(3) Substitution in the Axial Positions by More Electronegative Ligands Should Favor a Smaller Angle between the Equatorial Ligands. The reasoning here is as follows; decreasing the equatorial angle increases the electron density at the axial positions. Electronegative axial substituents take advantage of that accumulation of electron density, and so they will encourage a dimunition of the equatorial angle. Some experimental support for this is to be found in the structures in Table II. This trend has been noted by Paul, Martin, and Perozzi.[2b]

There is an interesting and totally different way to reach the third conclusion. Let's examine a potential energy surface for an SR_4 molecule in which C_{2v} symmetry is maintained and the equatorial and axial angles θ_1 and θ_2, as defined in **10**, are varied. Such a surface would be a two-di-

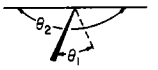

10

mensional slice through the five-dimensional surface that describes angular distortions in an SR_4 molecule with all bond lengths kept fixed. Figure 4 shows schematically the appearance of our two-dimensional slice. Note the presence of four (of the twelve total) equivalent minima, assumed to occur at idealized geometries $\theta_i = 105°$, $\theta_j = 180°$. The diagonal $\theta_1 = \theta_2$ represents square-pyramidal C_{4v} structures, while D_{2d} geometries lie on the other diagonal. Two tetrahedral geometries occur at special points on the latter diagonal, and the center of the diagram is the square-planar D_{4h} structure. Two Berry pseudorotations are marked by dashed lines. They are of much lower energy than another set of isomerizations which might proceed through the tetrahedral waypoints.

Consider now the effect of making two of the substituents, say the axial ones in **10**, more electronegative. Qualitatively we know the effect that substitution will have on the surface (the four minima will not remain of equal depth, but two of them, those with $\theta_2 = 180°$, $\theta_1 = 105°$, 255°, will become deeper than the other two). Very schematically the change is shown in **11** → **12**. Suppose we think of the

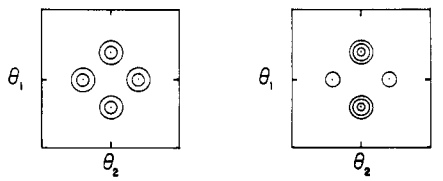

11 **12**

transformation from **11** to **12** as occurring by overlaying onto **11** a potential energy surface due to the perturbation. In principle the deepening of the two axial minima could be achieved by any of the three overlays **13–15.** In these diagrams + indicates a raise in energy due to substitution, ++ a greater raise, − a lowering in energy, etc. All energy changes are taken relative to a zero at the D_{4h} structure in

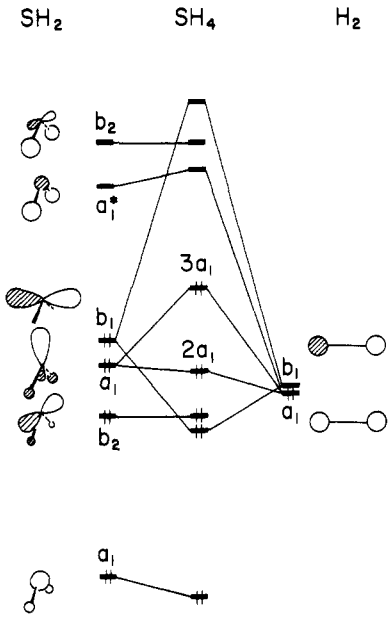

Figure 3. Interaction diagram for C_{2v} SH_4 constructed from the orbitals of SH_2 on the left and two axial hydrogens at right.

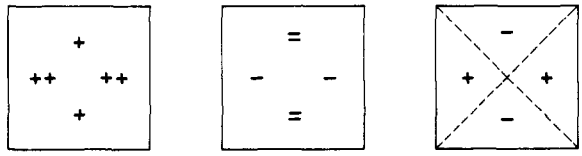

13 14 15

the center of the diagram. We would like to eliminate **13** on the basis that stabilization by one or more electronegative groups must have a stabilizing influence somewhere on the surface. It is difficult to decide between **14** and **15,** though we favor the latter. But we can proceed to a conclusion from either option.

If we take a slice of the surface of Figure 4 (or **11**) along the line $\theta_2 = 180°$, we will get a double minimum potential of the type shown in the dashed line of **16.** If the perturbation surface **14** or **15** is well behaved, a similar slice varying θ_1 at $\theta_2 = 180°$ will add on something like the dotted line of **16,** a contribution which is more negative as one moves away from $\theta_1 = 180°$. The important conclusion is that such a perturbation *must* have the effect of moving the position of the two minima along the θ_1 line further apart, i.e., to $\theta_1 < 105°$ and $\theta_1 > 255°$. In other words an increase in the electronegativity of the axial ligands has the effect of decreasing the equatorial angle, which is the conclusion reached previously.

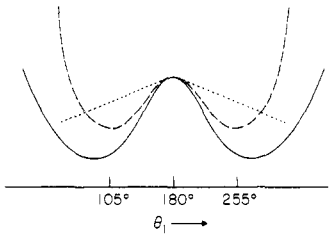

16

In principle we could distinguish between overlays **14** and **15** by comparing the structures of SR_4, $SR_2R'_2$, and SR'_4 where R′ is more electronegative than R. Both overlays **14** and **15** predict a reduction of the equatorial angle in $SR_2R'_2$ compared to SR_4. The symmetrically substituted SR'_4 can be thought of as being the product of a double overlay, with the second perturbation surface rotated by 90°. The difference between **14** and **15** arises because such a double overlay of the former would diminish the equatorial angle of SR'_4 further, while the latter would increase the equatorial angle in SR'_4 over that in $SR_2R'_2$. Unfortunately we do not find the structural data to make this decision. A final point concerning the "overlay" argument is that this mode of reasoning is applicable to the perturbation of any barrier problem by substituents. In particular it leads in an obvious manner to the correlation of increased pyramidality with increased inversion barrier in amines and phosphines.[11]

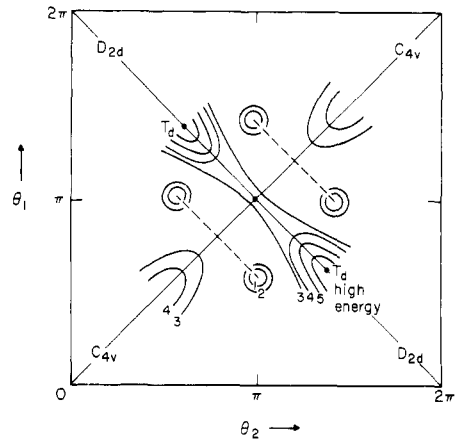

Figure 4. A model potential energy surface for SH_4, where the angles θ_1 and θ_2 are defined in **10.** The energy contours are schematic, meant only to indicate the primary features of a real surface. The four C_{2v} minima lie at θ_i approximately 105°, $\theta_j = 180°$. The diagonal $\theta_1 = \theta_2$ describes C_{4v} geometries, and D_{2d} structures lie along the line $\theta_1 = 2\pi - \theta_2$. Dashed lines mark two Berry pseudorotations.

Influencing the Axial Angle

There is no symmetry constraint on the axial angle θ_2, and indeed in the observed structures[2] it varies within a range of 10° to either side of the idealized trigonal bipyramid fragment value of 180°. The direction of axial ligand deformation observed in SF_4, **1,** is not unique, and structures have been found in which the axial ligands bend the other way, perhaps to be described as bending toward a tetrahedron rather than toward a square pyramid.

The simplest way to analyze how ligand electronegativity will influence the axial angle is to determine how the axial-equatorial charge differential in SH_4 is affected by changing θ_2. This is shown in Figure 5, for a fixed $\theta_1 = 120°$. Note that $\theta_2 = 180°$ is not a unique point, but that the disparity in axial and equatorial site electronic densities is increased as one increases θ_2 from 180°. The trend can be rationalized by a perturbation argument based on the mixing in of the a_1^* ($4a_1$) into the HOMO. From the charge imbalance we reason that the more disparate the electronegativity of the axial and equatorial ligands the greater θ_2. The structures studied to date are of little help in testing this conclusion. Either we are faced with large standard deviations in the structural parameters, or substituent pairs whose electronegativities are difficult to compare. Model calculations confirm the effect, but its magnitude is small. A greater accumulation of structural data is needed before one can decide if the theoretical prediction is correct.

Site Selectivity of Substituents with π-Donor or Acceptor Character

There are four extreme orientations that a substituent π-type orbital may assume, **17–20.** We probed the relative

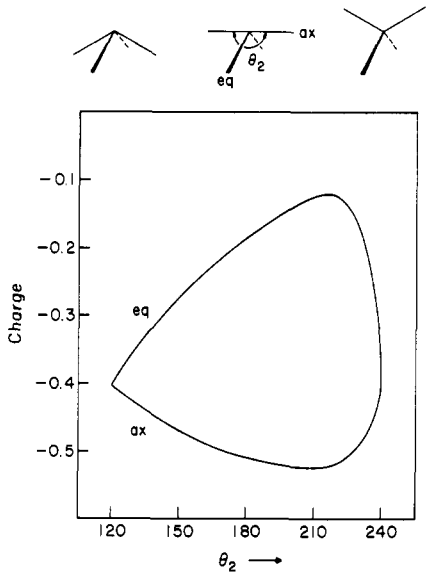

Figure 5. Atomic charge on the axial and equatorial hydrogens of SH_4, as θ_2 is varied at fixed θ_1. The angles are defined in **10.**

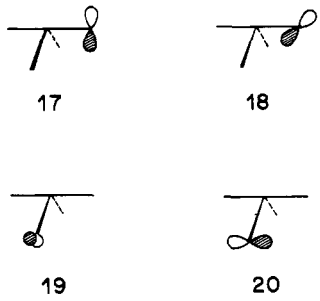

17 **18**

19 **20**

strength of interaction in these orientations by calculations with model substituents bearing a single p orbital, and with more realistic NH_2 and NO_2 groups.

In the phosphorane case our analysis had shown a differential π interaction for an equatorial substituent, with least interaction for an orientation analogous to **17.**[6] The interaction in question was with the framework σ orbitals of the phosphorane. In principle the same interactions are present in the sulfurane, except that superimposed on them is a new interaction with a high-lying, directional lone pair on sulfur. Our calculations indicate that interactions with this lone pair, mainly $2a_1$, but to some extent in $3a_1$ as well, dominate the conformational preferences of donors and acceptors. In the usual way acceptors should seek to maximize interaction with this lone pair, while donors might strive to minimize it. The calculations confirm this. Thus acceptor orbitals prefer **17** to **18** and **19** to **20,** while donors have reversed preferences. This is without 3d orbitals on S. When these are included, with parameters yielding an exaggerated degree of mixing, the situation is less clear cut. In particular in the case of a model SH_3NH_2 with 3d orbitals conformation **19** is calculated as being more stable than **20.** The stabilization of **19** is presumably due to better ligand-framework π bonding in the equatorial plane, a factor previously analyzed in the phosphorane case.[6] We do not trust, however, the computational result, since the energy of the 3d orbitals is put unrealistically low in our calculation. It is clear that in an equatorial SR_3NR_2 two competing effects would be operating: a tendency for the S and N lone pairs to avoid each other, favoring **20,** and an opposing tendency to maximize p-d π bonding favoring **19.** Structural studies of such sulfuranes would be of great interest.

Table III. Parameters Used in Extended Hückel Calculations

Orbital	H_{ii}	Slater exponent
S 3s	−20.0	2.122
S 3p	−11.0	1.827
S 3d	−8.0	1.500
F 2s	−40.0	2.425
F 2p	−18.1	2.425
H 1s	−13.6	1.300
N 2s	−26.0	1.950
N 2p	−13.4	1.950
O 2s	−32.3	2.275
O 2p	−14.8	2.275

Experimental structures of sulfuranes containing π-donor or acceptor substituents are sparse. $SF_3N(CH_3)_2$ has been synthesized, and its NMR spectrum is consistent with equatorial substitution.[23] No information on its orientation is available. The synthesis and structure of a diaryldialkoxysulfurane have been reported.[2b] The conformation which best avoids interactions of the sulfurane lone pair with the σ and p lone pairs of each OR group is that shown in **21.**

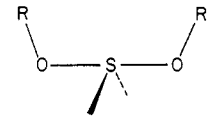

21

In the crystal structure both OR groups are oriented approximately in that fashion. It should be noted that a spirosulfurane which cannot achieve this conformation is nevertheless a remarkably stable compound.[24]

Acknowledgment. We are grateful to Rolf Gleiter and Notker Rösch for communicating to us their work prior to publication. Our research at Cornell was generously supported by the National Science Foundation and by the Advanced Research Projects Agency through the Materials Science Center at Cornell University.

Appendix

The calculations were of the extended Hückel type,[25] based on idealized SH_4 and SF_4 geometries. The basic S-H and S-F distances were 1.35 and 1.59 Å, and were set equal for axial and equatorial bonds. The C_{2v} structures were idealized to a fragment of a trigonal bipyramid, with an equatorial XSX angle of 120° and an axial XSX angle of 180°. In the study of substituent effects the following distances were used: S-N 1.60, S-O 1.90, N-H 1.01, O-H 0.96, N-O 1.24 Å. The extended Hückel parameters are summarized in Table III.

As usual in our calculations we set the energy of the S 3d orbitals, when they were used, low. We also contracted the 3d functions so that they interacted in a way that simulated strong 3d participation. Where it was desired to simulate a more electronegative ligand than hydrogen, a pseudoatom was defined with the 1s orbital of hydrogen, but with a Coulomb integral lowered to −14.6 eV.

References and Notes

(1) The structure was determined by electron diffraction and microwave spectroscopy: K. Kimura and S. H. Bauer, *J. Chem. Phys.*, **39,** 3172 (1963); V. C. Ewing and L. E. Sutton, *Trans. Faraday Soc.*, **59,** 1241 (1963); W. M. Tolles and W. D. Gwinn, *J. Chem. Phys.*, **36,** 1119 (1962).
(2) In the examples we list here, which are not exhaustive, we have excluded those which exhibit a molecular complex, $SR_2 \cdot X_2$, structure in the crystal. Some of the Se and Te compounds show in the solid varying degrees of association such that the environment at the group 6 atom approaches octahedral coordination. (a) Bis(2-carboxyphenyl)sulfur dihydroxide dilactone, $S(OCO(C_6H_4))_2$: I. Kapovits and A. Kalman,

Chem. Commun., 649 (1971); A. Kalman, K. Sasvari, and I. Kapovits, *Acta Crystallogr., Sect. B*, **29**, 335 (1971). (b) $(C_6H_5)_2S(OC(CF_3)_2C_6H_5)_2$: I. C. Paul, J. C. Martin, and E. F. Perozzi, *J. Am. Chem. Soc.*, **93**, 6674 (1971); *ibid.*, **94**, 5010 (1972). (c) $Cl_2S(C_6H_4Cl)_2$: N. C. Baenziger, R. E. Buckles, R. J. Maner, and T. D. Simpson, *ibid.*, **91**, 5749 (1969). (d) $Cl_2Se(C_6H_5)_2$ and $Br_2Se(C_6H_5)_2$: J. D. McCullough and G. Hamburger, *ibid.*, **64**, 508 (1942). (e) $Cl_2Se(p\text{-}C_6H_4CH_3)_2$ and $Br_2Se(p\text{-}C_6H_4CH_3)_2$: J. D. McCullough and R. E. Marsh, *Acta Crystallogr.*, **3**, 41 (1950). (f) $TeCl_4$: D. P. Stevenson and V. Schomaker, *J. Am. Chem. Soc.*, **62**, 1267 (1940). (g) $Br_2Te(C_6H_5)_2$: G. D. Christofferson and J. D. McCullough, *Acta Crystallogr.*, **11**, 249 (1958). (h) $I_2Te(p\text{-}C_6H_4Cl)_2$: G. Y. Chao and J. D. McCullough, *ibid.*, **15**, 887 (1962). (i) $Cl_2Te(CH_3)_2$: G. D. Christofferson, R. A. Sparks, and J. D. McCullough, *ibid.*, **11**, 782 (1958). (j) $I_2Te(C_{12}H_8O)$: J. D. McCullough, *Inorg. Chem.*, **12**, 2669 (1973). (k) $I_2Te(C_{12}H_8)$: J. D. McCullough, *ibid.*, **14**, 1142 (1975). (l) $I_2Te(C_4H_8O)$: H. Hope, C. Knobler, and J. D. McCullough, *ibid.*, **12**, 2665 (1973). (m) $I_2Te(C_4H_8S)$: C. Knobler, J. D. McCullough, and H. Hope, *ibid.*, **9**, 797 (1970). (n) $Br_2Se(C_4H_8S)$: L. Bateile, C. Knobler, and J. D. McCullough, *ibid.*, **6**, 958 (1967). (o) $Cl_2SeC_4H_8SeCl_2$: A. Amendola, E. S. Gould, and B. Post, *ibid.*, **3**, 1199 (1964). (p) $Br_2Te(C_4H_8S)$: C. Knobler and J. D. McCullough, *ibid.*, **11**, 3026 (1972).

(3) E. L. Muetterties and R. A. Schunn, *Q. Rev., Chem. Soc.*, **20**, 245 (1966).

(4) This is discussed in many of the structural papers in ref 2. For example in $Br_2Se(C_6H_5)_2$ the axial Se–Br bonds are 2.52 (1) Å while the sum of the covalent radii is only 1.17 + 1.14 = 2.31 Å. In contrast the equatorial Se–C bonds are normal, 1.91 (3) Å compared with the sum of the covalent radii of 1.17 + 0.772 = 1.94 Å.

(5) (a) R. J. Hach and R. E. Rundle, *J. Am. Chem. Soc.*, **73**, 4321 (1951); R. E. Rundle, *ibid.*, **85**, 112 (1963); R. E. Rundle, *Surv. Prog. Chem.*, **1**, 81 (1963); (b) G. C. Pimentel, *J. Chem. Phys.*, **19**, 446 (1951); (c) E. E. Havinga and E. H. Wiebenga, *Recl. Trav. Chim. Pays-Bas*, **78**, 724 (1959); (d) R. J. Gillespie, *Inorg. Chem.*, **5**, 1634 (1966); *J. Chem. Phys.*, **37**, 2498 (1962); *Can. J. Chem.*, **39**, 318 (1961); (e) J. I. Musher, *Angew. Chem.*, **81**, 68 (1969); (f) K. J. Wynne, "Sulfur Research Trends", Mardi Gras Symposium, 3d, Loyola University, 1971, p 150.

(6) An extensive list of references may be found in the paper by R. Hoffmann, J. M. Howell, and E. L. Muetterties, *J. Am. Chem. Soc.*, **94**, 3047 (1972).

(7) (a) R. D. Willett, *Theor. Chim. Acta*, **2**, 393 (1964); (b) D. P. Santry and G. A. Segal, *J. Chem. Phys.*, **47**, 158 (1967); D. P. Santry, *J. Am. Chem. Soc.*, **90**, 3309 (1968); M. Keeton and D. P. Santry, *Chem. Phys. Lett.*, **7**, 105 (1970); (c) R. D. Brown and J. B. Peel, *Aust. J. Chem.*, **21**, 2589, 2605, 2617 (1968); (d) R. M. Gavin, Jr., *J. Chem. Educ.*, **46**, 413 (1969); (e) A. L. Companion, *Theor. Chim. Acta*, **25**, 268 (1970); (f) J. I. Musher and V. B. Koutecky, *ibid.*, **33**, 227 (1974); (g) G. M. Schwenzer and H. F. Schaeffer, III, *J. Am. Chem. Soc.*, **97**, 1391 (1975); L. Radom and H. F. Schaeffer, III, *Aust. J. Chem.*, **28**, 2069 (1975); (h) R. Gleiter and A. Veillard, *Chem. Phys. Lett.*, **37**, 33 (1976); (i) N. Rösch, V. H. Smith, Jr., and M. H. Whangbo, to be published; (j) V. I. Minkin and R. M. Minyaev, *Zh. Org. Khim.*, **11**, 1993 (1975); (k) M. Albeck and S. Schaik, *J. Chem. Soc., Perkin Trans. 1*, 1223 (1975).

(8) A detailed discussion of the electronic structure of PH_4 and phosphoranyl radicals in general is given by J. M. Howell, Brooklyn College, to be published. The tetrahedral structure is used as a departure point in this work.

(9) R. Hoffmann, R. W. Alder, and C. F. Wilcox, Jr., *J. Am. Chem. Soc.*, **92**, 4992 (1970).

(10) B. M. Gimarc, *J. Am. Chem. Soc.*, **93**, 593 (1971).

(11) A similar argument has been elegantly applied in a study of the pyramidalization of amines: C. C. Levin, *J. Am. Chem. Soc.*, **97**, 5649 (1975).

(12) R. Hoffmann, *Acc. Chem. Res.*, **4**, 1 (1971); L. Libit and R. Hoffmann, *J. Am. Chem. Soc.*, **96**, 1370 (1974), and references therein.

(13) A comparison should note the difference in the numbering of the levels: $4a_1$ of ref 7g is our $1a_1$, $2b_2$ is our $1b_2$, etc.

(14) L. S. Bartell and R. M. Gavin, Jr., *J. Chem. Phys.*, **48**, 2466 (1968).

(15) (a) R. G. Pearson, *J. Am. Chem. Soc.*, **91**, 4947 (1969); (b) Pearson, on the basis of a different level scheme for SF_4, does find a reason for such a distortion.

(16) O. Foss and K. Maroy, *Acta Chem. Scand.*, **15**, 1945 (1961); O. Foss, K. Maroy and S. Husebye, *ibid.*, **19**, 2361 (1965); K. Fosheim, O. Foss, A. Scheie, and S. Solheimsnes, *ibid.*, **19**, 2336 (1965); O. Foss, H. M. Kjoge, and K. Maroy, *ibid.*, **19**, 2349 (1965), and other work by the same group.

(17) L. S. Bartell and K. W. Hansen, *Inorg. Chem.*, **4**, 1777 (1965); K. W. Hansen and L. S. Bartell, *ibid.*, **4**, 1775 (1965); L. S. Bartell, *ibid.*, **5**, 1635 (1966); L. S. Bartell, *J. Chem. Educ.*, **45**, 754 (1968).

(18) D. R. Johnson and F. X. Powell, *Science*, **164**, 950 (1969).

(19) H. A. Bent, *Chem. Rev.*, **61**, 275 (1961).

(20) A. D. Walsh, *Discuss. Faraday Soc.*, *2*, 18 (1947); *Trans. Faraday Soc.*, **42**, 56 (1946); *ibid.*, **43**, 60, 158 (1947); *Proc. R. Soc. A*, **207**, 13 (1951).

(21) O. Hassel and H. Viervoll, *Acta Chem. Scand.*, **1**, 149 (1947); H. J. Dothie, *Acta Crystallogr.*, **6**, 804 (1953); R. E. Marsh, *ibid.*, **8**, 91 (1955).

(22) R. E. Marsh and J. D. McCullough, *J. Am. Chem. Soc.*, **73**, 1106 (1951).

(23) G. C. Demitras and A. G. MacDiarmid, *Inorg. Chem.*, **6**, 1903 (1967).

(24) E. F. Perozzi, J. C. Martin, and I. C. Paul, *J. Am. Chem. Soc.*, **96**, 6735 (1974).

(25) R. Hoffmann, *J. Chem. Phys.*, **39**, 1397 (1963); R. Hoffmann and W. N. Lipscomb, *ibid.*, **36**, 2179, 3489; **37**, 2872 (1962).

The Least-Motion Insertion Reaction $CH_2(^1A_1) + H_2 \rightarrow CH_4$. Theoretical Study of a Process Forbidden by Orbital Symmetry[1a]

Charles W. Bauschlicher, Jr.,[1b] Henry F. Schaefer III,*[1b] and Charles F. Bender[1c]

Contribution from the Department of Chemistry and Lawrence Berkeley Laboratory,[1d] University of California, Berkeley, California 94720, and Lawrence Livermore Laboratory,[1d] University of California, Livermore, California 94550. *Received May 21, 1975*

Abstract: Ab initio electronic structure theory has been applied to the insertion reaction of singlet methylene with molecular hydrogen. Since the molecular orbital descriptions of $CH_2(^1A_1) + H_2$ and CH_4 differ by two electrons, the least-motion approach considered here is forbidden in the sense of Woodward and Hoffmann. Electron correlation was explicitly taken into account via configuration interaction (CI). The CI included all singly and doubly excited configurations (a total of 1192) with respect to three reference configurations. A primary goal was the location of the saddle point or transition state (within the constraints of the least motion approach adopted) geometry with $R = 2.20$ Å, $r = 0.76$ Å, and $\theta = 172°$. This stationary point on the potential energy surface lies 26.7 kcal/mol above separated $CH_2(^1A_1) + H_2$. The portion of the minimum energy path near the saddle point has been obtained by following the gradient of the potential energy in the direction of most negative curvature. The electronic structure at the transition state is compared with that of the reactants and product in terms of the natural orbitals resulting from the wave functions.

In the time since the 1965 publication by Woodward and Hoffmann of their landmark communications,[2] the concept of orbital symmetry has taken on tremendous importance in organic chemistry. The purpose of the present paper is to report a detailed theoretical study of a simple Woodward–Hoffmann forbidden process: the least-motion insertion of singlet methylene into H_2 to yield methane. This pathway is shown qualitatively in Figure 1. There it is seen that C_{2v} symmetry is arbitrarily imposed on the five atoms, whose positions are uniquely defined by the specification of the three geometrical parameters R, r, and θ. An ab initio correlation diagram for

$$CH_2(^1A_1) + H_2(^1\Sigma_g^+) \rightarrow CH_4(^1A_1) \qquad (1)$$